EUROPEAN ORGANIZATION FOR NUCLEAR RESEARCH

CERN/SPSC/78-96
SPSC/P 110/Add.1
17 August 1978

Appendix to the Proposal

STUDY OF π^-p INTERACTIONS WITH NEUTRAL FINAL STATES: PRELIMINARY EXPERIMENTAL RESULTS WITH GAMS

IHEP[1]-IISN[2]-LAPP[3] Collaboration

F.G. Binon[2], C. Bricman[2], Yu.B. Bushnin[1], V.A. Davidov[1], S.V. Donskov[1],
J. Dufournaud[3], M. Gouanère[3], A.V. Inyakin[1], D.T. Jayanti[2], V.A. Kachanov[1],
D.B. Kakauridze[1], G.V. Khaustov[1], A.V. Kulik[1], J.P. Lagnaux[2],
A.A. Lednev[1], Yu.V. Mikhailov[1], J.P. Peigneux[3], Yu.D. Prokoshkin[1],
R. Roosen[2], S.A. Sadovsky[1], V.A. Senko[1], D. Sillou[3], M. Spighel[3],
A.V. Starzev[1], J.P. Stroot[2], A.N. Sytin[1]

---

1) Institute for High-Energy Physics, Serpukhov, USSR.
2) Institut Interuniversitaire des Sciences Nucléaires, Bruxelles, Belgium.
3) Laboratoire d'Annecy de physique des particules, France.

1. INTRODUCTION

In Spring 1978 the GAMS-200 spectrometer was assembled and used in an experiment at the 70 GeV IHEP accelerator as a first phase in the realization of the GAMS program described earlier$^{1)}$.

The set-up (Fig. 1) is a small-scale copy of GAMS-4000 $^{2)}$. Besides the beam counters and beam hodoscopes, the three main parts of the system are the following: a) a liquid hydrogen target which permits to locate the interaction point by measuring the Cerenkov light intensity of the incident particle; b) a guard system consisting of scintillation counters and lead-glass counters in order to select the candidates for the charge-exchange reactions; c) the GAMS-200 hodoscope assembly. To study the antiproton charge-exchange reaction at small t-values by means of a hadron calorimeter, a study which is part of the GAMS-200 project, an auxiliary sweeping magnet has been added to the set-up.

The standard lead-glass cells for GAMS-200, as well as for the guard system, are identical to the ones foreseen for the GAMS-4000 system (Fig. 2). The data-taking system for the GAMS-200 spectrometer is less elaborate than that foreseen for GAMS-4000 and, furthermore, the ADC chains were taken over from an older experiment (NICE)$^{3)}$. However, the monitoring and calibration procedures are completely similar to those proposed for GAMS-4000. These and the first experimental results with GAMS-200 will be enlarged upon in some detail.

2. CALIBRATION AND MONITORING

The GAMS-200 counters were precalibrated and continuously monitored with light-emitting diodes (LEDs). All light pulses, originating from a common source and comparable in amplitude to a 25 GeV electromagnetic shower, are distributed to each cell through low absorption optical fibre light-guides. The width of the pulse amplitude distribution is 2 to 3% . The homogeneity of the characteristics of the counters is such that the dispersion of photomultiplier high voltages is less than 10%.

The stability of the system is controlled to a 1% level by a systematic comparison of the LED pulse magnitude with pulses from a scintillator irradiated by a standard α source (Am or Pu) on a reference photomultiplier. No significant drift has been observed during the running period (Figs. 3a and b).

Energy calibration of GAMS-200 was made both with muons and electrons.

In the first case, the whole set-up was irradiated with a wide muon beam. The mean amplitude of the muon signal is equivalent to that delivered by a 0.7 GeV electron shower. The FWHM of muon pulses was 25%.

The calibration with electrons was made in two ways. Firstly, a 3 × 3 mm^2 area around the centre of each counter was irradiated by a pencil beam. The spectrometer was moved across the beam on a movable platform and located with a precision of better than 1 mm. Secondly, the total area of about 16 counters was simultaneously irradiated with a defocused beam. The electrons were in both cases identified with threshold Cerenkov counters (hadron contamination less than 1%). The results of both methods agree to 1%. The former calibration took five hours, while the latter required only two hours.

The ratio of the mean values of the electron to muon signals A_e/A_μ practically does not vary from one counter to another within the precision limits determined by the linearity and the stability of the ADCs (Fig. 4). It means that the technically simpler calibration with muons may be used to control and calibrate the spectrometer within 10% precision.

3. EXPERIMENTAL RESULTS

Systematic studies of the reactions

$$\pi^- p \to \pi^0 n \quad (\pi^0 \to 2\gamma) \tag{1}$$

and

$$\pi^- p \to \eta^0 n \quad (\eta^0 \to 2\gamma) \tag{2}$$

at 25 GeV/c and 40 GeV/c incident π^- momenta have been started. The main aim of these first runs was to establish the GAMS working conditions and its characteristics in a real experiment.

A total of 50000 π^0's from reaction (1) and 1000 η's from reaction (2) were collected in June 1978. Samples of these data are presented in the following figures as they were *displayed on-line* with a HP 2100 computer.

Figure 5 represents a typical π^0 event.

Figure 6 shows the distribution of triggered events as a function of the total energy deposited in GAMS. The peak corresponds to the "elastic" two-body processes (1). The lead-glass guard counter signals were not brought into the trigger. This information was used at a later stage of the on-line analysis.

The observed mass of the "elastic" events, as obtained through application of the method of moments to the amplitudes in individual cells, already shows a clear discrimination of reaction (1) (Fig. 7). The low-energy peak mainly contains events where only one γ is visible. This is substantiated by Fig. 8, which shows the same distribution for those events where two γ's are clearly distinguished.

Using a rather simple algorithm for reconstructing the individual showers and for determining their position and energy, the effective mass $M_{eff} = (E_{\gamma_1}E_{\gamma_2})^{1/2}\ \theta_{\gamma\gamma}$, where $\theta_{\gamma\gamma}$ is the laboratory angle between the two γ's, has been evaluated for the same events (Fig. 9). At this stage of the analysis there is already no measurable background (<< 1%).

The $\theta_{\gamma\gamma}$ angular distribution of π^0 events is characteristic for a two-body decay (Fig. 10). The fast slope of the distribution to the left of θ_{min} is due to the high precision of the γ-ray coordinate measurement ($\lesssim$ 1.5 mm). The π^0 azimuthal angular distribution is isotropic (Fig. 11).

The cos θ^* distribution, where θ^* is the decay angle in the π^0 centre-of-mass system, indicates a loss of events at small angles, which is due to the geometrical acceptance of the set-up (Fig. 12).

The π^0 energy curve given in Fig. 13 is somewhat wider than expected from GAMS resolution [formula (2) in Ref. 1], because no on-line calibration and drift corrections were performed at this stage.

Figure 14 shows the mass spectrum of 2γ events with $\chi^2 \leq 2.5$ after a 1C-fit to reaction (1) at 25 GeV/c π^- momentum. The π^0 peak has a FWHM of 5 MeV. The standard deviation

$$\sigma_M/M_{\pi^0} = 1.5 \times 10^{-2} \tag{3}$$

is definitely smaller than the one obtained heretofore with total absorption γ spectrometers. For comparison, the mass spectrum including the η region, obtained immediately after assembling GAMS, before its calibration (the LED signals were visually equalized on the oscilloscope), is shown in Fig. 15.

Finally the t-dependence of the differential cross-section for reaction (1) at small t is shown in Fig. 16, as determined on-line without acceptance correction.

4. GAMS-50

A small (compared to GAMS-4000) γ-ray spectrometer GAMS-50 made of fifty GAMS-type lead-glass hodoscope cells has been associated with the IHEP muon magnetic spectrometer in a search for rare meson decays ("lepton-G" set-up) with the participation of a few members of the GAMS group.

The experiment$^{4)}$, which was concluded in the Spring of 1978, has led to the first observation of the η decay channel $\eta \to \mu^+\mu^-\gamma$. The measured branching ratio is $BR(\eta \to \mu^+\mu^-\gamma) = 1.5 \times 10^{-4}$.

Figure 17 shows the mass spectrum of the $\mu^+\mu^-\gamma$ systems produced in 25 GeV/c π^-p collisions. A peak containing 100 events, after 15% background subtraction, is seen. Its mean mass value agrees with the tabulated η mass value up to 2%, an error which can be assigned to systematic effects.

This was really the first use of a GAMS-type spectrometer in a large experiment. It gave the opportunity to solve the problem of precise coordinate and energy measurement in GAMS also in the presence of two mesons traversing it simultaneously. It has also been the first successful GAMS reliability test as it has been working during 2000 hours, in a beam of 4×10^6 particles per second.

5. CONCLUSIONS

GAMS-200 preliminary experimental results confirm the conclusions which were made on the basis of the former tests and measurements with electron beams$^{2)}$.

GAMS cellular structure allows an easy coordinate evaluation, thus yielding the momentum vector of each γ-ray directly. In this way simple on-line analysis already gives a rather precise overview of the physics involved. This is not so with magnetic spectrometers or with NICE-type γ-ray spectrometers where the trajectory of the particle has to be determined from two independent projections in plane detectors.

For particles with large masses, a mass resolution of better than 10^{-2} can be achieved at SPS with GAMS-4000.

For practical purposes it is worth emphasizing that the large GAMS-4000 spectrometer can be calibrated with muons in 12 hours and with electrons in two days. Scaling up from GAMS-200 to GAMS-4000 should not raise any problem. The LED source for the monitoring system, which has reliably performed, can be used for a thousand counters. Only four of them will be needed for GAMS-4000 and they will together provide further cross-checking. The reliability shown by GAMS-50 is confirmed by the 1000 hours of use of the more than three hundred GAMS-200 counters (including the guard system) without breakdown.

REFERENCES

1) G.A. Akopdjanov et al., IHEP preprint 77-3 (1977).

2) F. Binon et al., CERN/SPSC/78-95, SPSC/P 110 (1978).

3) Yu.B. Bushnin et al., IHEP preprint 74-21 (1974); Nuclear Instrum. Methods 120, 391 (1974).

4) Yu.B. Bushnin et al., Observation of decay $\eta \to \mu^+\mu^-\gamma$, IHEP preprint 78-110 (1978).

Figure captions

Fig. 1 : GAMS-200 experimental set-up in the 40 GeV/c π^- beam at IHEP.

Fig. 2 : GAMS-200 spectrometer and guard system counters. In the background are shown lead-glass blocks for GAMS-4000.

Fig. 3 : a) Stability of the system including the light diodes, the photomultiplier, the high voltage supply and the ADC after switching on. A short power switch-off is indicated by a pointer.

b) Same as Fig. 3a, but after some hours of running.

Fig. 4 : Ratio of the mean amplitudes of electron and muon pulses at 25 GeV/c.

Fig. 5 : Typical π^0 event. The two display views are rotated through 90° to each other.

Fig. 6 : Spectrum of the total energy deposited in GAMS for the triggered events. The pointer shows the beam energy.

Fig. 7 : Mass spectrum of "elastic" events as calculated by the method of moments.

Fig. 8 : Mass spectrum of "elastic" events with two visible γ-rays.

Fig. 9 : Effective mass spectrum of "elastic" events.

Fig. 10 : Distribution as a function of $\theta_{\gamma\gamma}$, the decay angle. $\theta_{min} = 2m_\pi/E$ is the minimum π^0 decay angle.

Fig. 11 : Azimuthal angle ϕ distribution.

Fig. 12 : Distribution of cos θ^*, the decay angle in the π^0 c.m. system.

Fig. 13 : π^0 energy spectrum.

Fig. 14 : Mass spectrum of the γ pairs after a 1C-fit of the events to the reaction (1).

Fig. 15 : Mass spectrum of events for both reactions (1) and (2) before spectrometer calibration.

Fig. 16 : Display view of the t-dependence of the differential cross-section for reaction (1). $0 \le |t| < 0.3$ (GeV/c)^2.

Fig. 17 : $\mu^+\mu^-\gamma$ mass spectrum. The peak corresponds to the decay $\eta \to \mu^+\mu^-\gamma$.

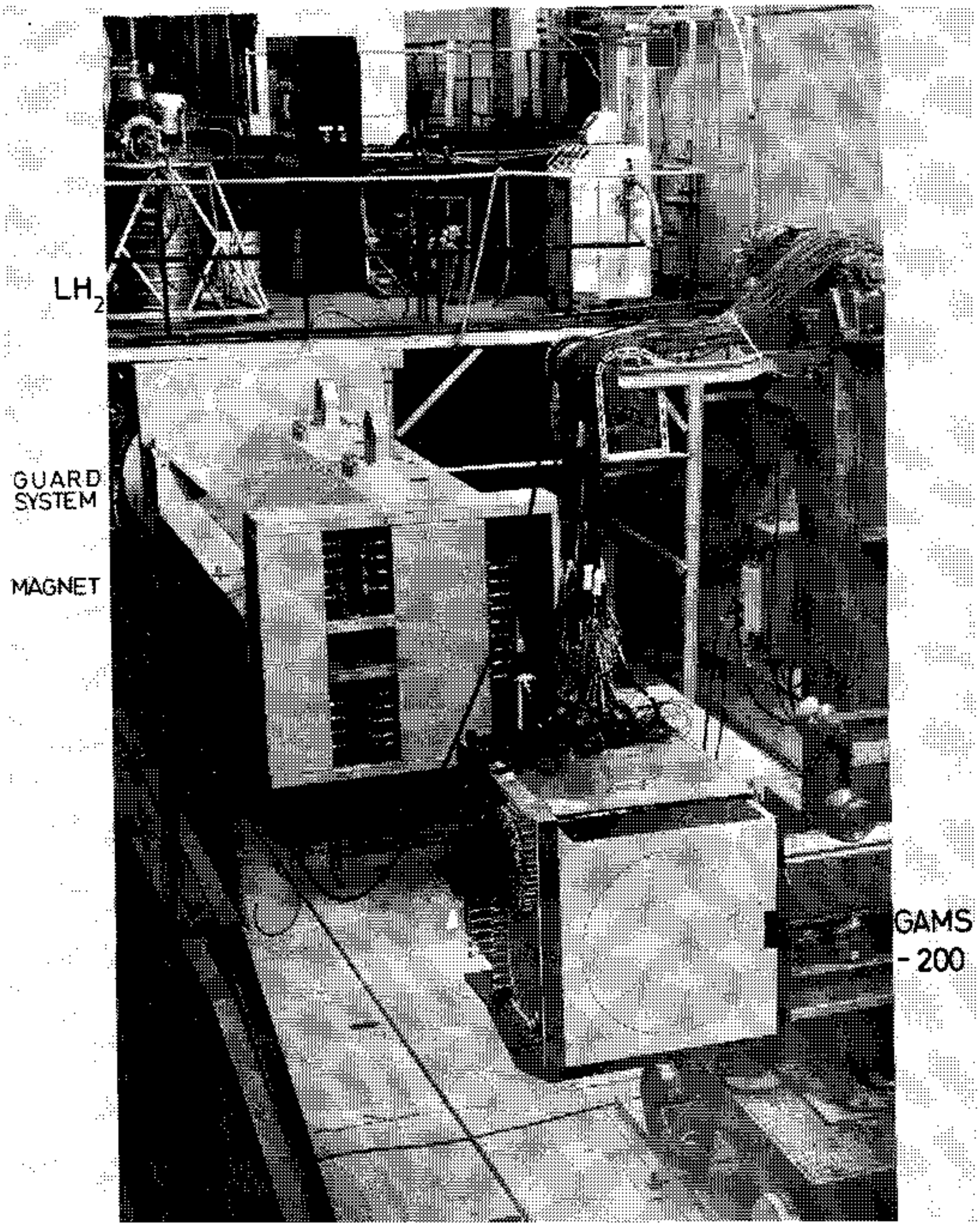

Fig. 1

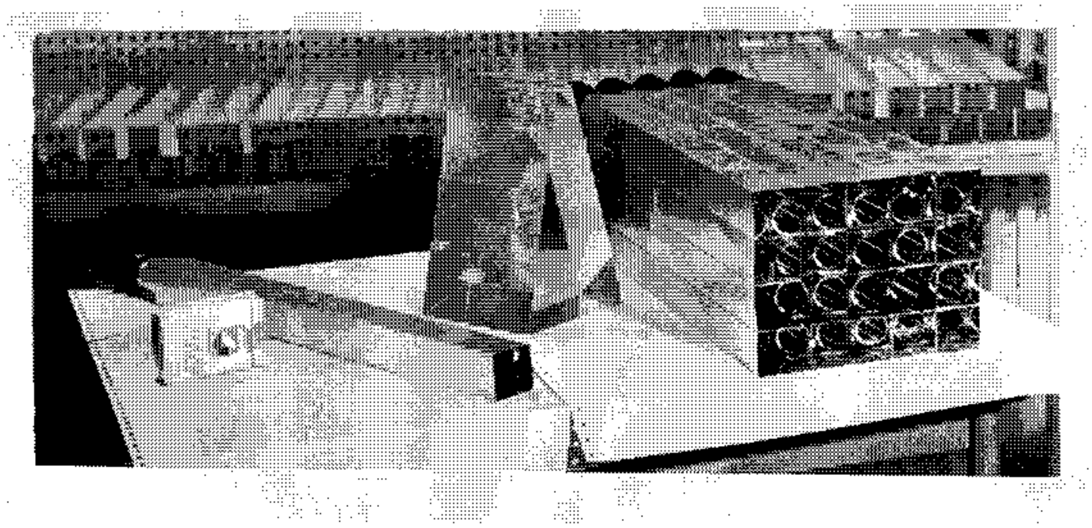

Fig. 2

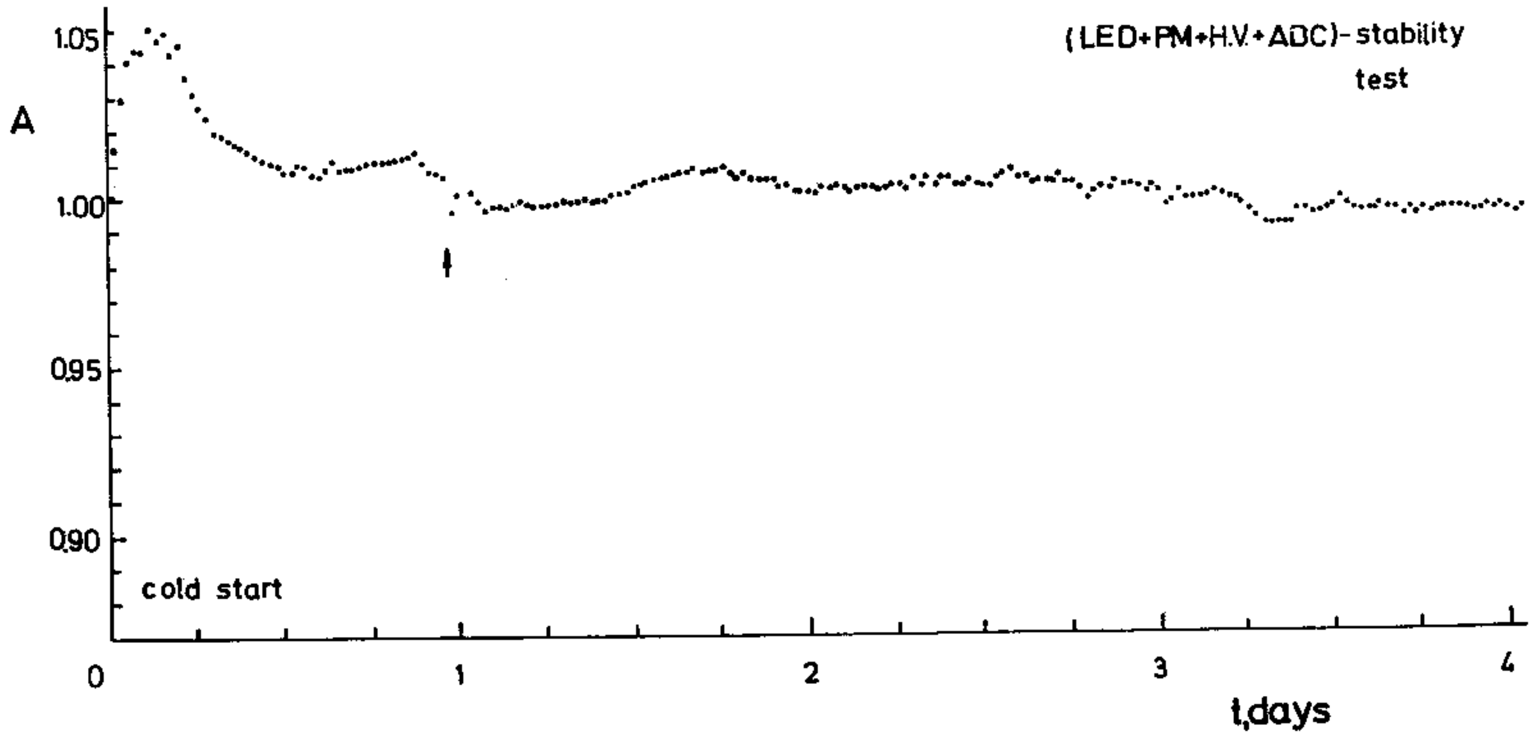
(LED+PM+H.V.+ADC)-stability
test
A
1.05
1.00
0.95
0.90
cold start
0
1
2
3
4
t,days

Fig. 3a

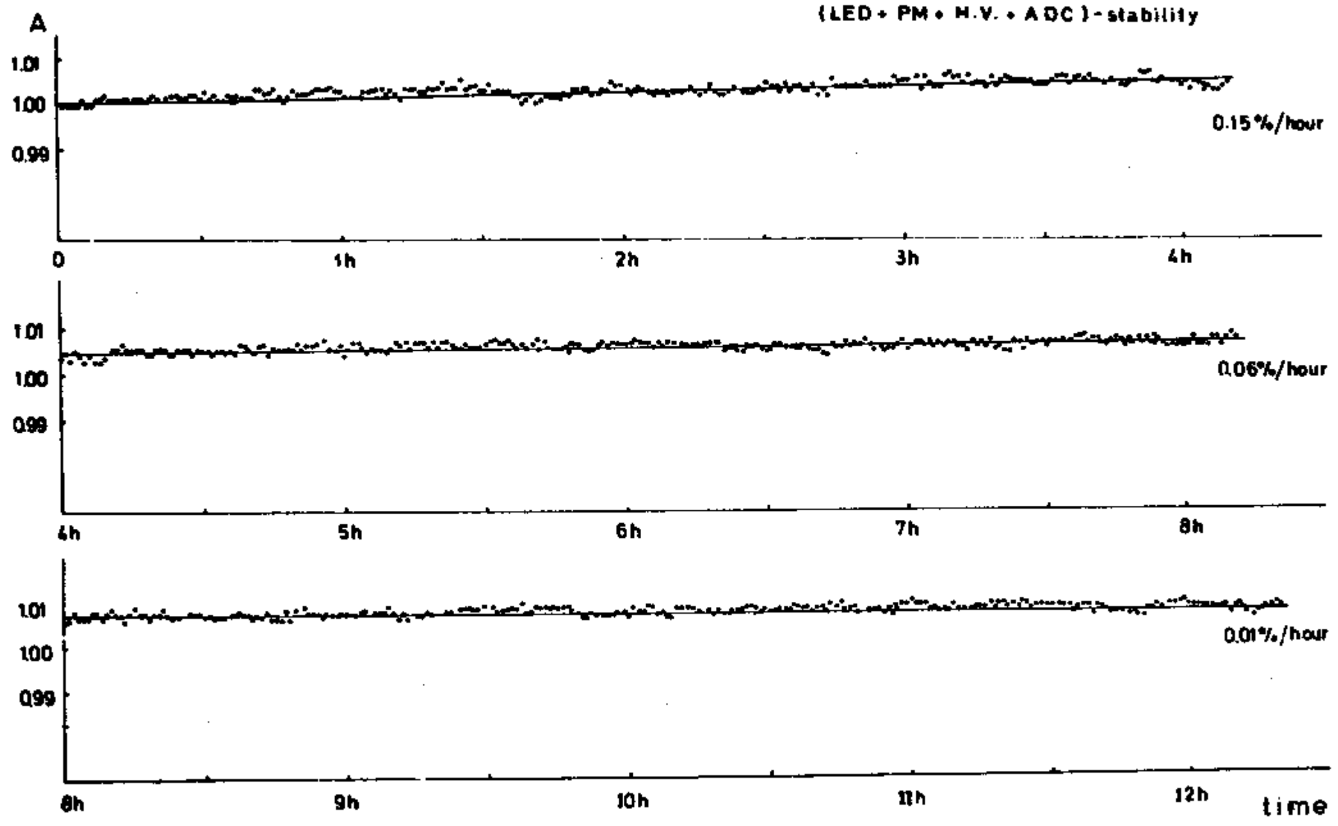
(LED + PM + H.V. + ADC)-stability
A
1.01
1.00
0.99
0.15%/hour
0
1h
2h
3h
4h
1.01
1.00
0.99
0.06%/hour
4h
5h
6h
7h
8h
1.01
1.00
0.99
0.01%/hour
8h
9h
10h
11h
12h
time

Fig. 3b

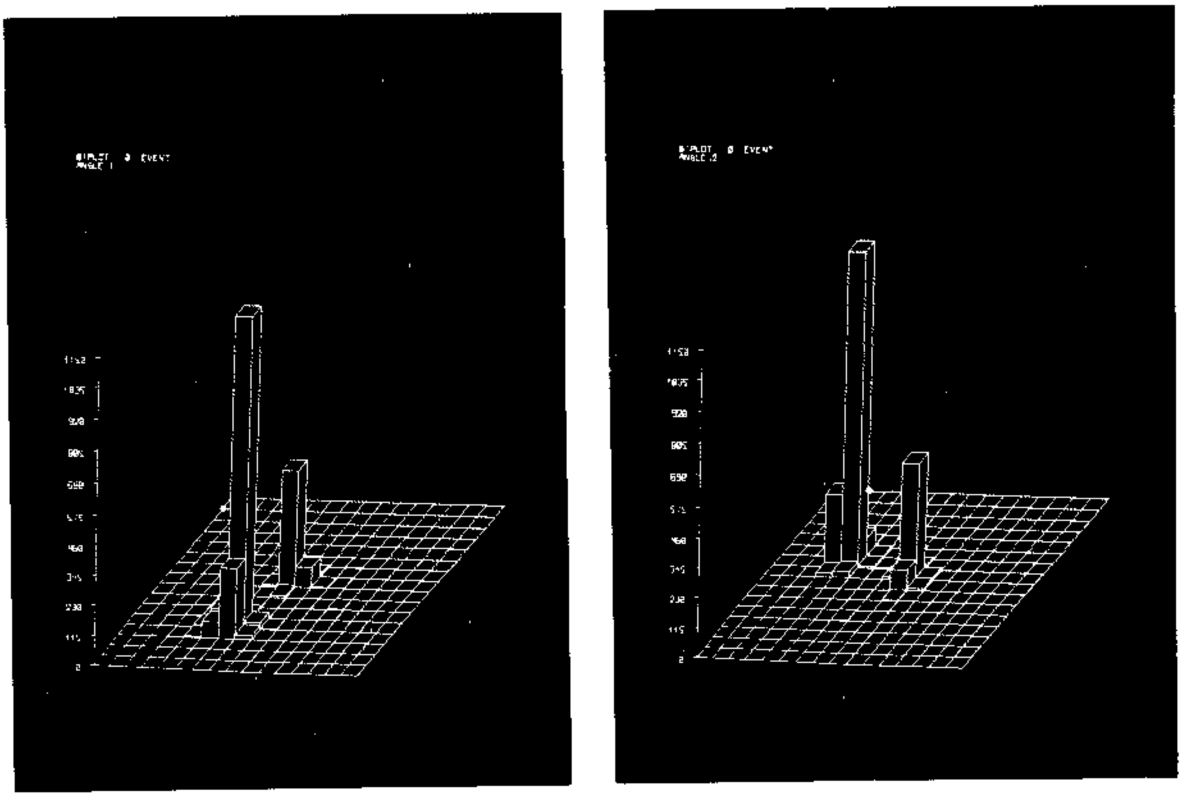
BIPLOT 0 EVENT
ANGLE 1
1150
1035
920
805
690
575
460
345
230
115
0
BIPLOT 0 EVENT
ANGLE 2
1150
1035
920
805
690
575
460
345
230
115
0

Fig. 5

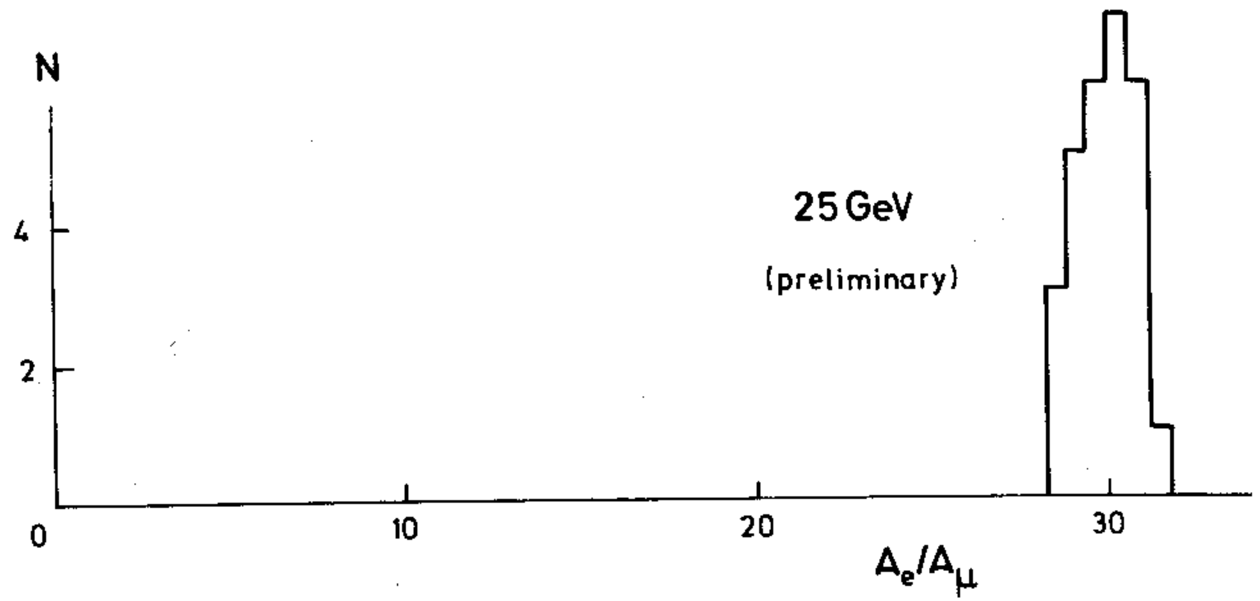

Fig. 4

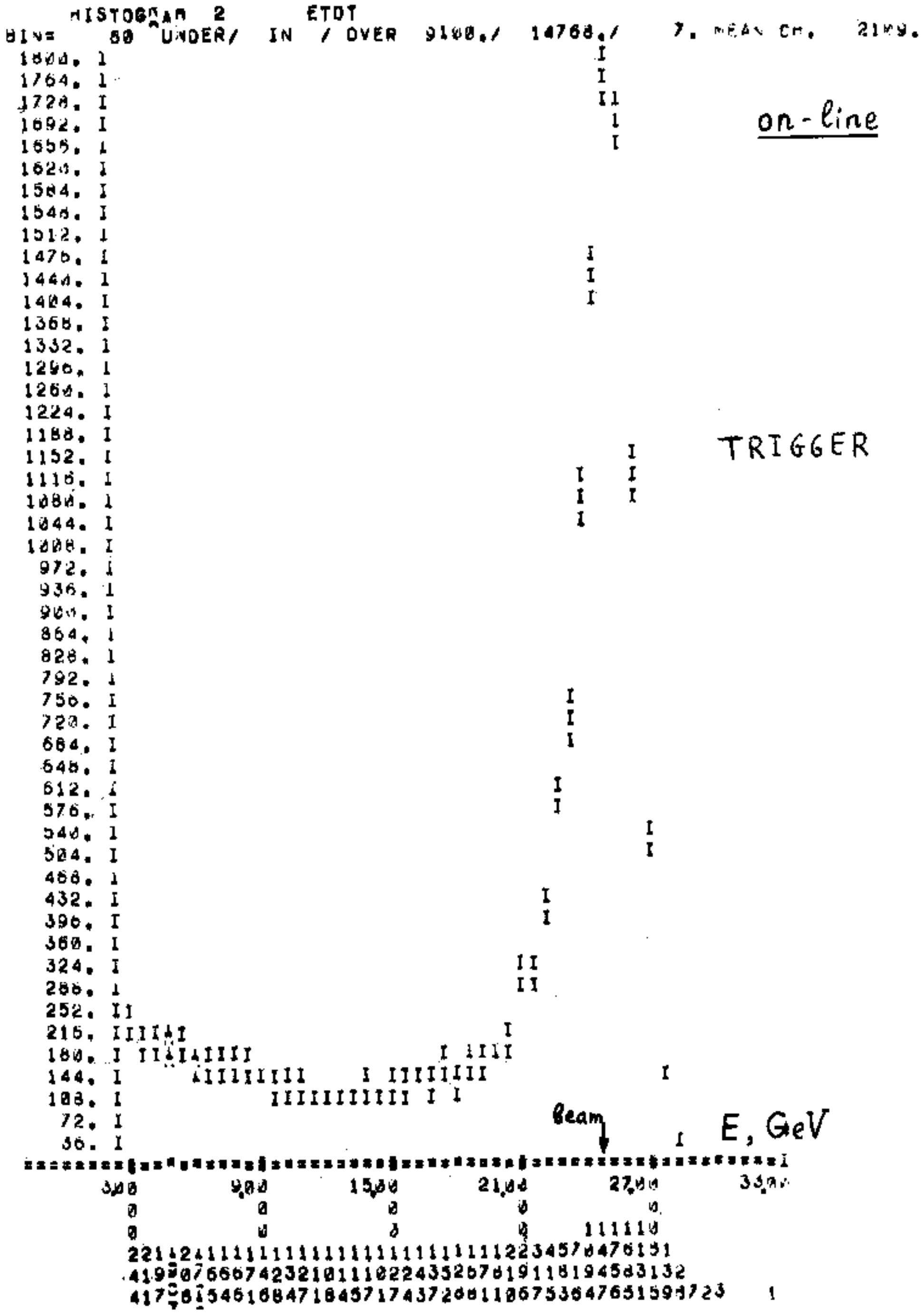
HISTOGRAM 2 ETOT
BIN= 60 UNDER/ IN / OVER 9100./ 14768./ 7. MEAN CH. 2199.
on-line
TRIGGER
Beam
E, GeV
1800.
1764.
1728.
1692.
1656.
1620.
1584.
1548.
1512.
1476.
1440.
1404.
1368.
1332.
1296.
1260.
1224.
1188.
1152.
1116.
1080.
1044.
1008.
972.
936.
900.
864.
828.
792.
756.
720.
684.
648.
612.
576.
540.
504.
468.
432.
396.
360.
324.
288.
252.
216.
180.
144.
108.
72.
36.
300
900
1500
2100
2700
3300

Fig. 6

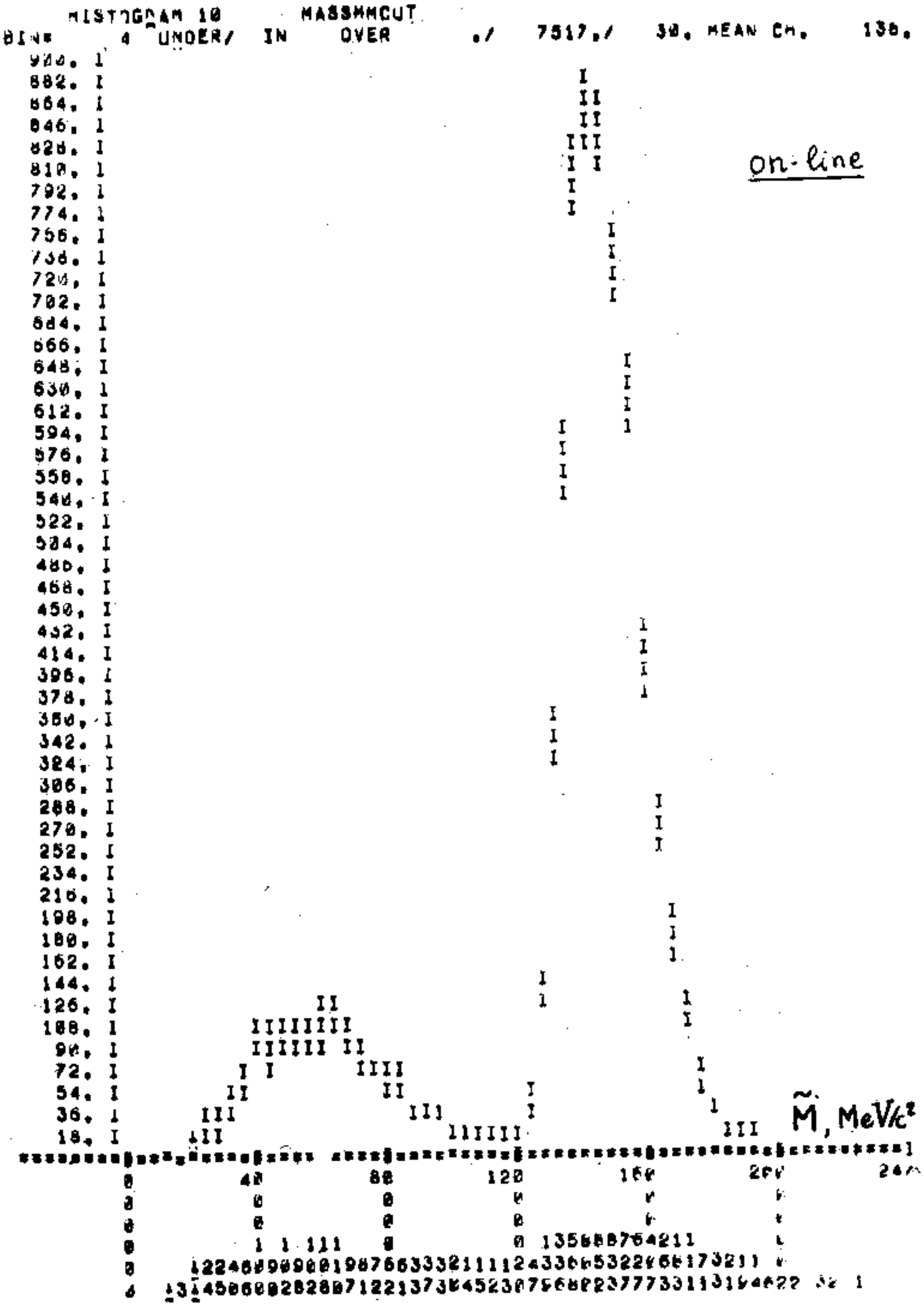
HISTOGRAM 10 MASSMMCUT
BIN= 4 UNDER/ IN OVER ./ 7517./ 30. MEAN CH. 136.
on-line
M̃, MeV/c²
0
40
80
120
160
200
240

Fig. 7

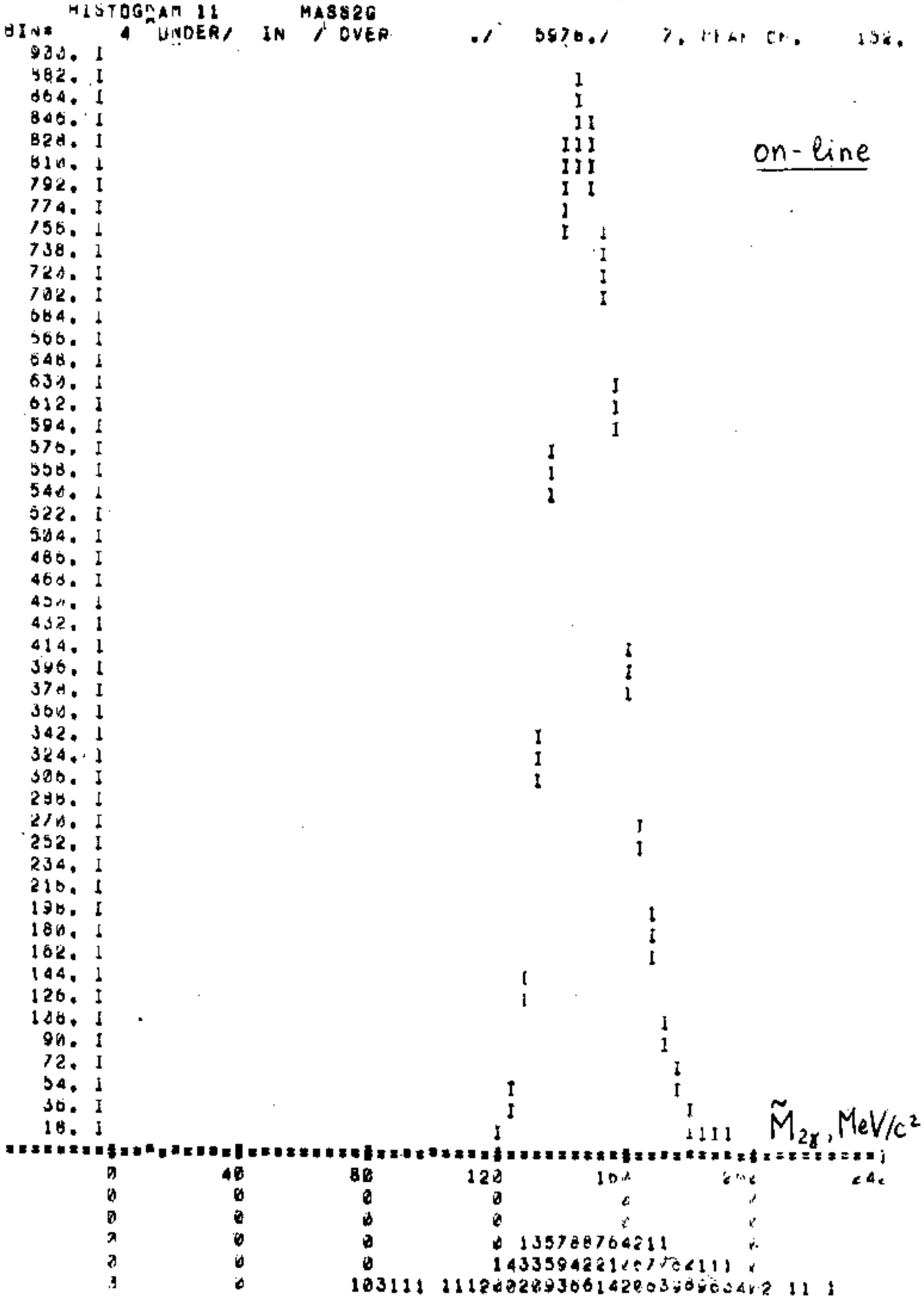
HISTOGRAM 11 MASS2G
BIN* 4 UNDER/ IN / OVER ./ 5976./ 7, PEAK CH. 152.
on-line
$\tilde{M}_{2\gamma}$, MeV/c²
0
40
80
120
160
200
240

Fig. 8

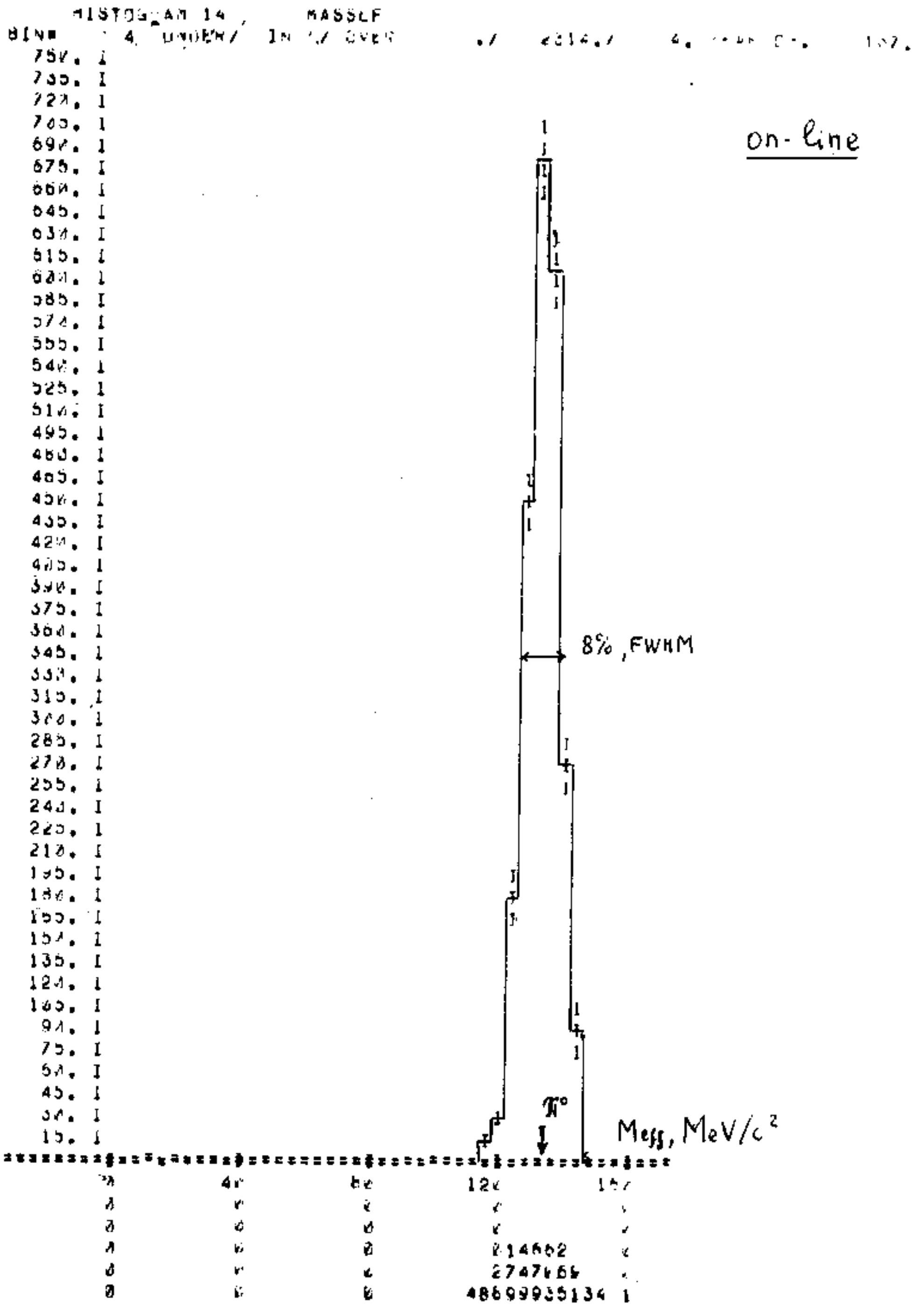
HISTOGRAM 14 , MASSEF
BIN=
on-line
750.
735.
720.
705.
690.
675.
660.
645.
630.
615.
600.
585.
570.
555.
540.
525.
510.
495.
480.
465.
450.
435.
420.
405.
390.
375.
360.
345.
330.
315.
300.
285.
270.
255.
240.
225.
210.
195.
180.
165.
150.
135.
120.
105.
90.
75.
60.
45.
30.
15.
8%, FWHM
π°
Meff, MeV/c²
120
214662
2747666
48699935134

Fig. 9

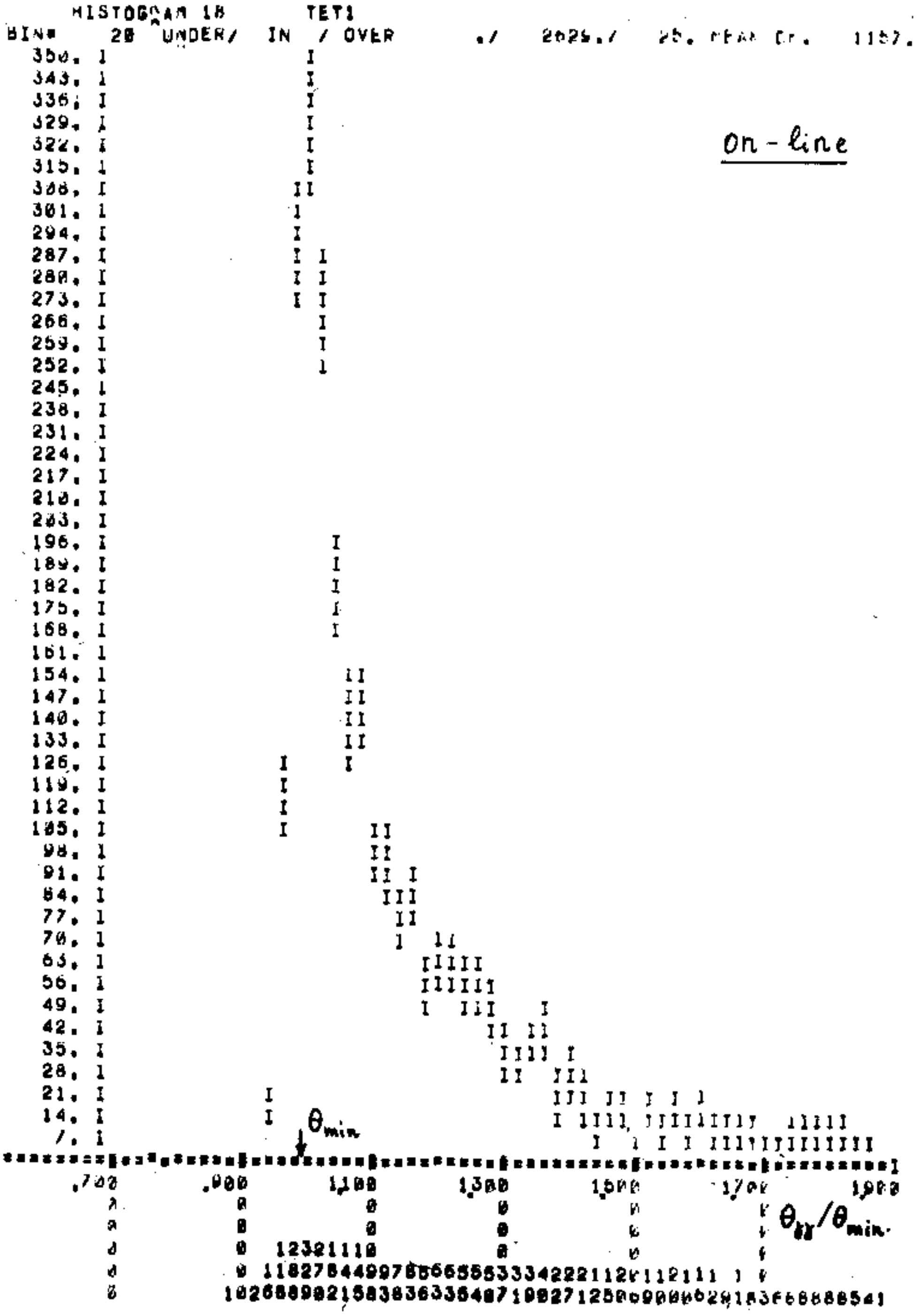
HISTOGRAM 18 TET1
BIN# 20 UNDER/ IN / OVER ./ 2025./ 25. PEAK CT. 1157.
On-line
350.
343.
336.
329.
322.
315.
308.
301.
294.
287.
280.
273.
266.
259.
252.
245.
238.
231.
224.
217.
210.
203.
196.
189.
182.
175.
168.
161.
154.
147.
140.
133.
126.
119.
112.
105.
98.
91.
84.
77.
70.
63.
56.
49.
42.
35.
28.
21.
14.
7.
θ_{min}
.700
.900
1.100
1.300
1.500
1.700
1.900
$\theta_{lab}/\theta_{min}$

Fig. 10

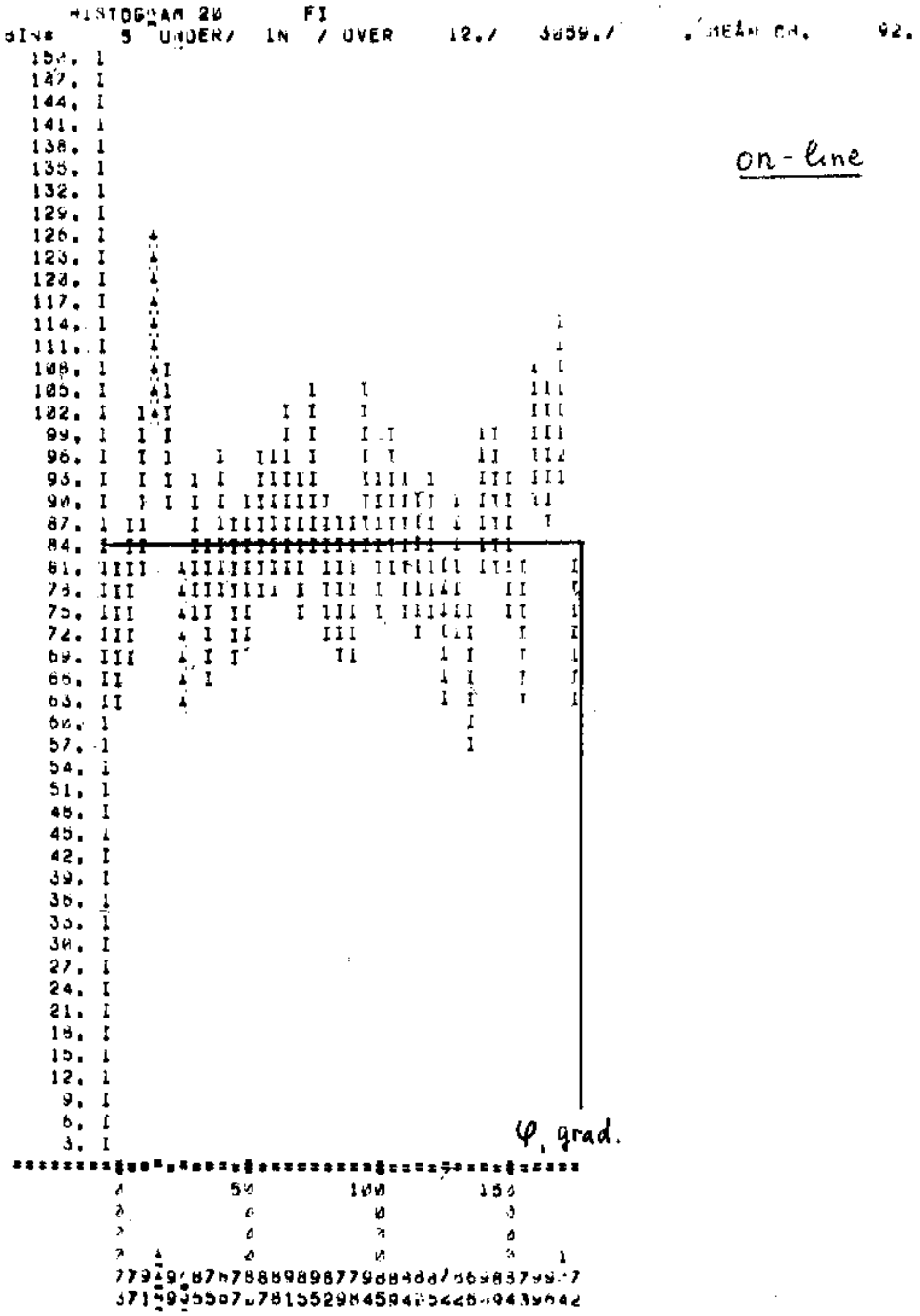

HISTOGRAM 20 FI
BINS 5 UNDER/ IN / OVER 12./ 3859./ MEAN CH. 92.
on-line
φ, grad.
0
50
100
150
3.
6.
9.
12.
15.
18.
21.
24.
27.
30.
33.
36.
39.
42.
45.
48.
51.
54.
57.
60.
63.
66.
69.
72.
75.
78.
81.
84.
87.
90.
93.
96.
99.
102.
105.
108.
111.
114.
117.
120.
123.
126.
129.
132.
135.
138.
141.
144.
147.
150.

Fig. 11

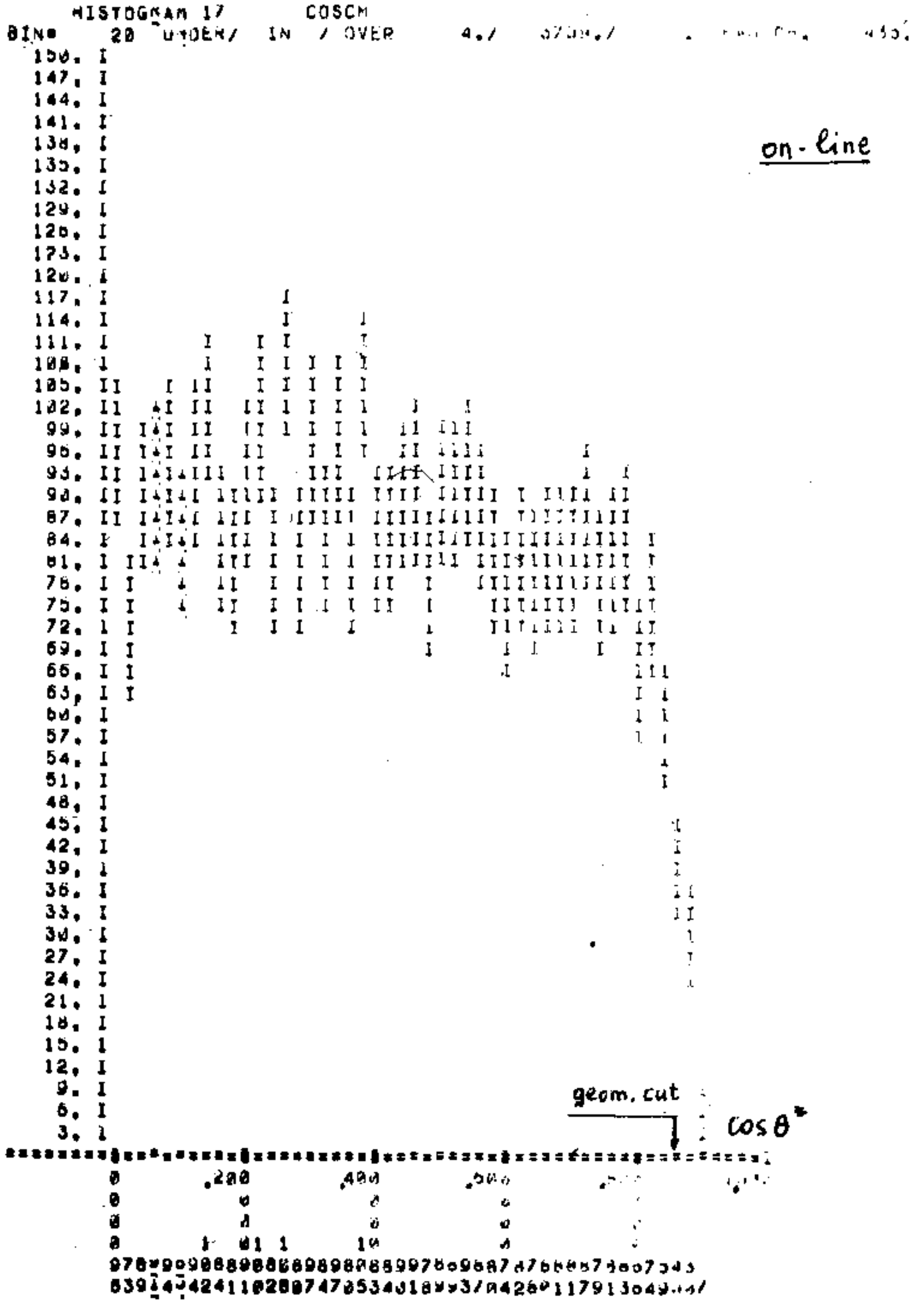
HISTOGRAM 17
COSCM
BIN
UNDER/ IN / OVER
150.
147.
144.
141.
138.
135.
132.
129.
126.
123.
120.
117.
114.
111.
108.
105.
102.
99.
96.
93.
90.
87.
84.
81.
78.
75.
72.
69.
66.
63.
60.
57.
54.
51.
48.
45.
42.
39.
36.
33.
30.
27.
24.
21.
18.
15.
12.
9.
6.
3.
0
.200
.400
on-line
geom. cut
cos θ*

Fig. 12

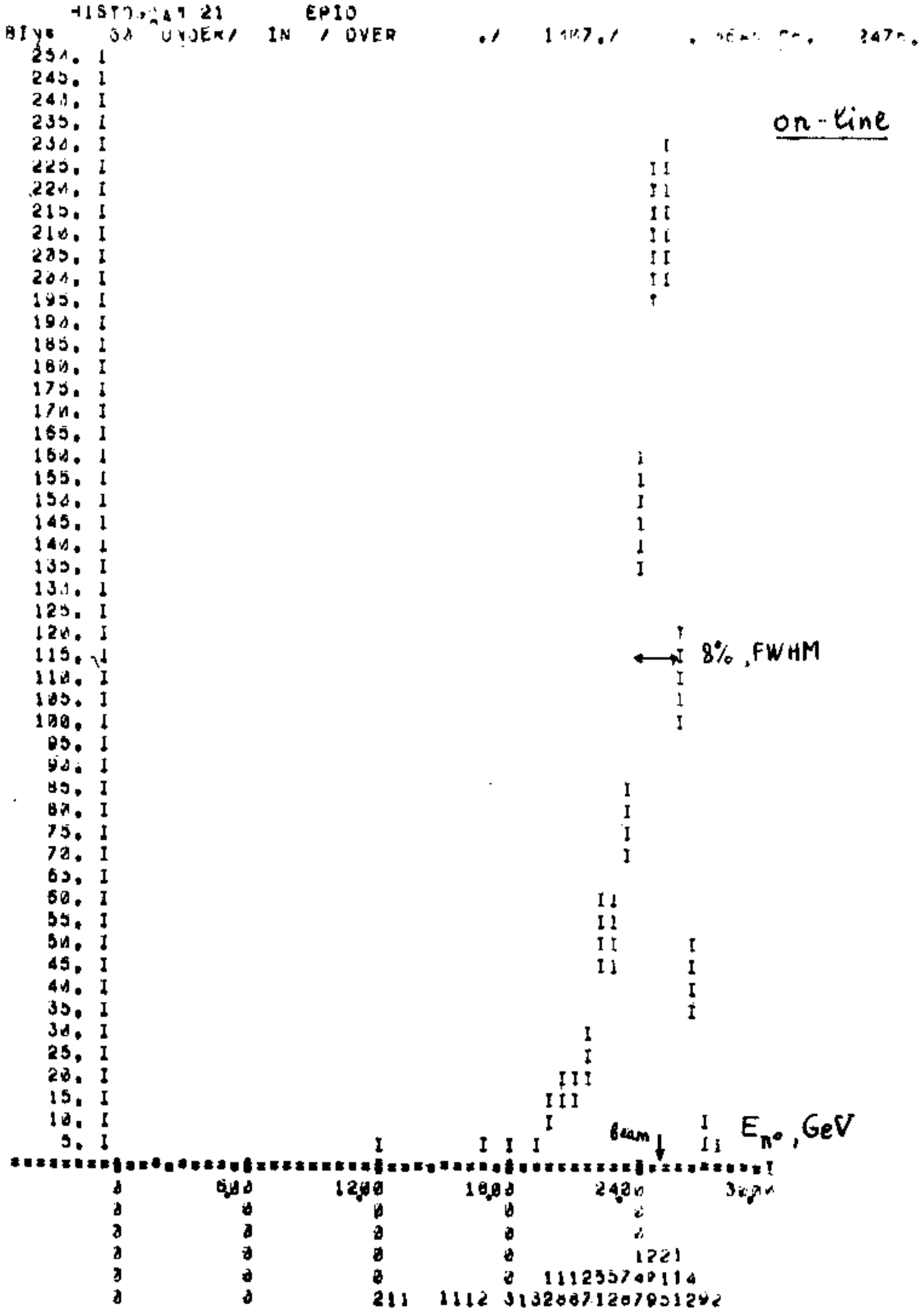
HISTOGRAM 21 EPIO
BINS UNDER/ IN / OVER
on-line
8% ,FWHM
Beam
E_{π^0} ,GeV
250.
200.
150.
100.
50.
5.
0
600
1200
1800
2400
3000

Fig. 13

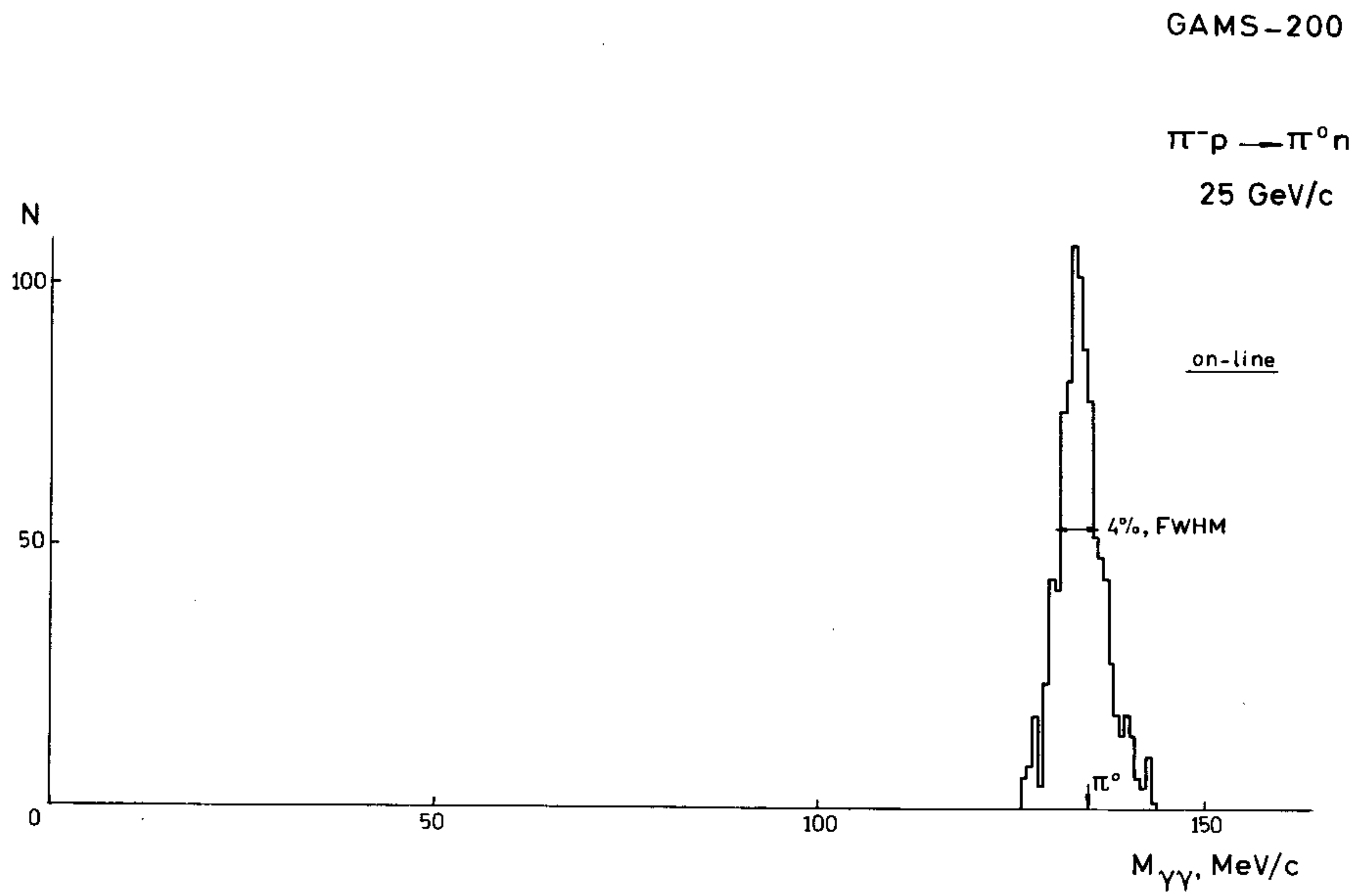
GAMS-200
$\pi^- p \rightarrow \pi^0 n$
25 GeV/c
on-line
4%, FWHM
π^0
N
100
50
0
50
100
150
$M_{\gamma\gamma}$, MeV/c

Fig. 14

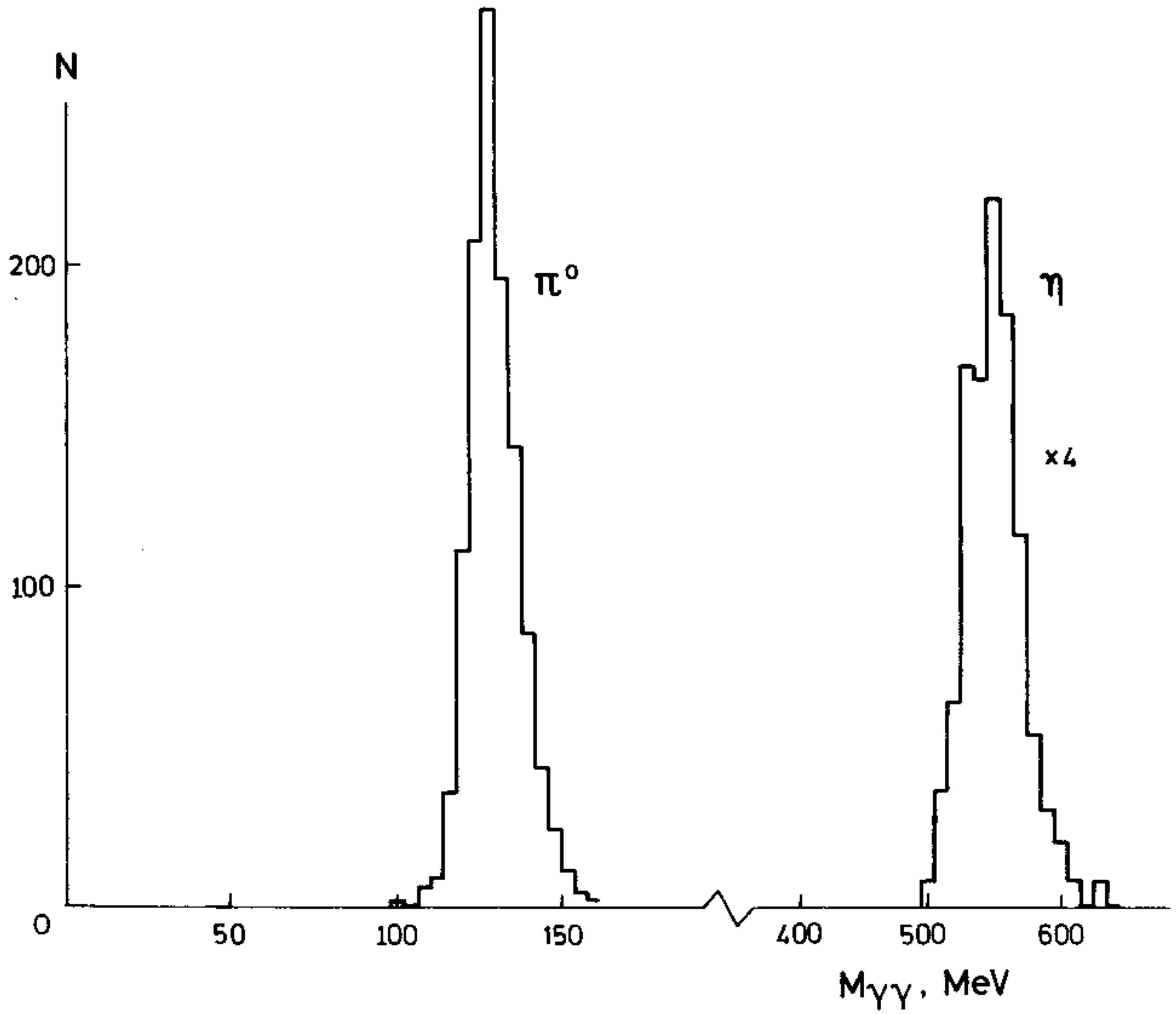

GAMS - 200

15 June 1978

(FIRST DATA, WITHOUT
CALIBRATION, TAKEN
FROM DISPLAY)

Fig. 15

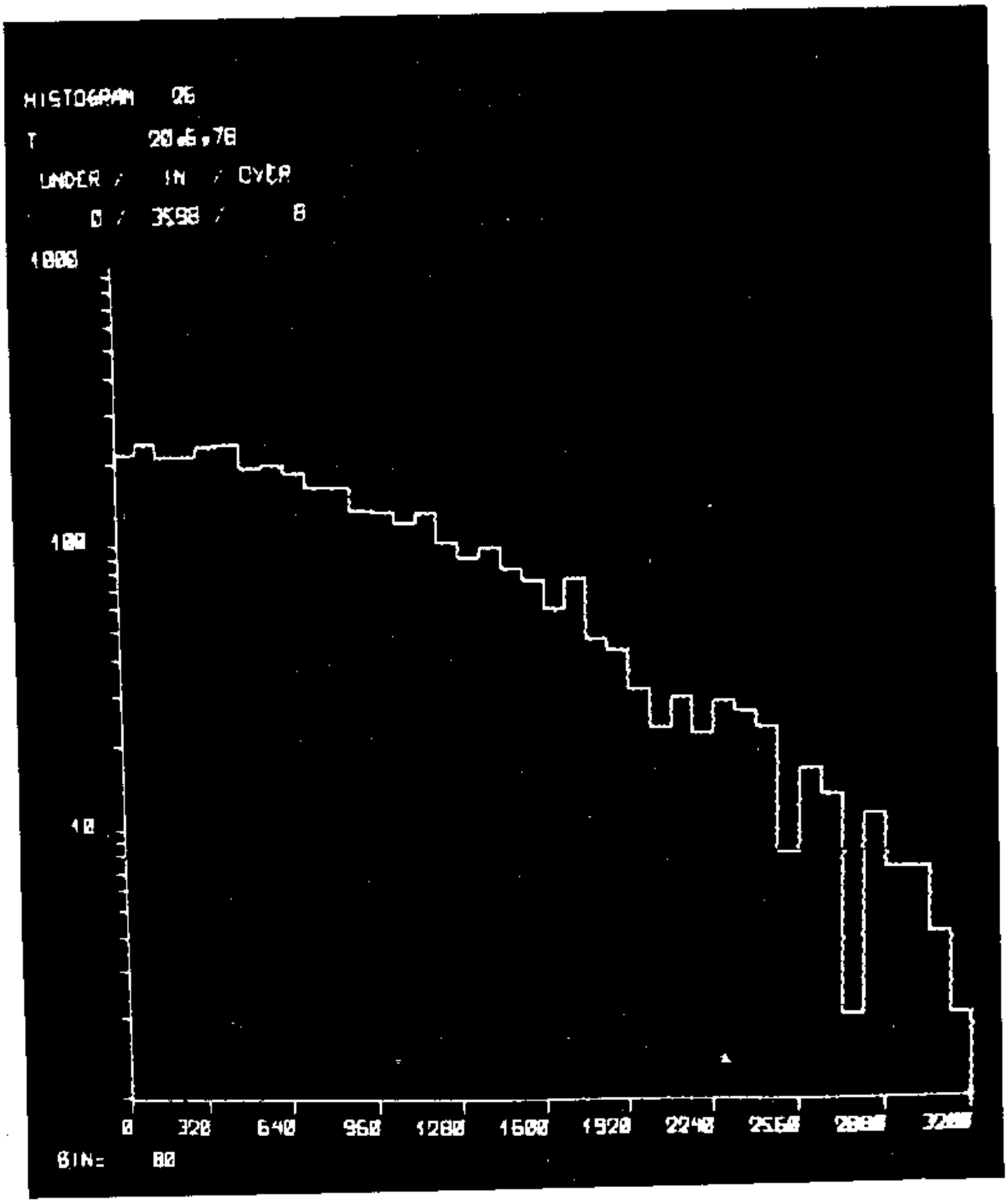
HISTOGRAM 26
T 20.6.78
UNDER / IN / OVER
0 / 3598 / 8
1000
100
10
0
320
640
960
1280
1600
1920
2240
2560
2880
3200
BIN= 80

Fig. 16

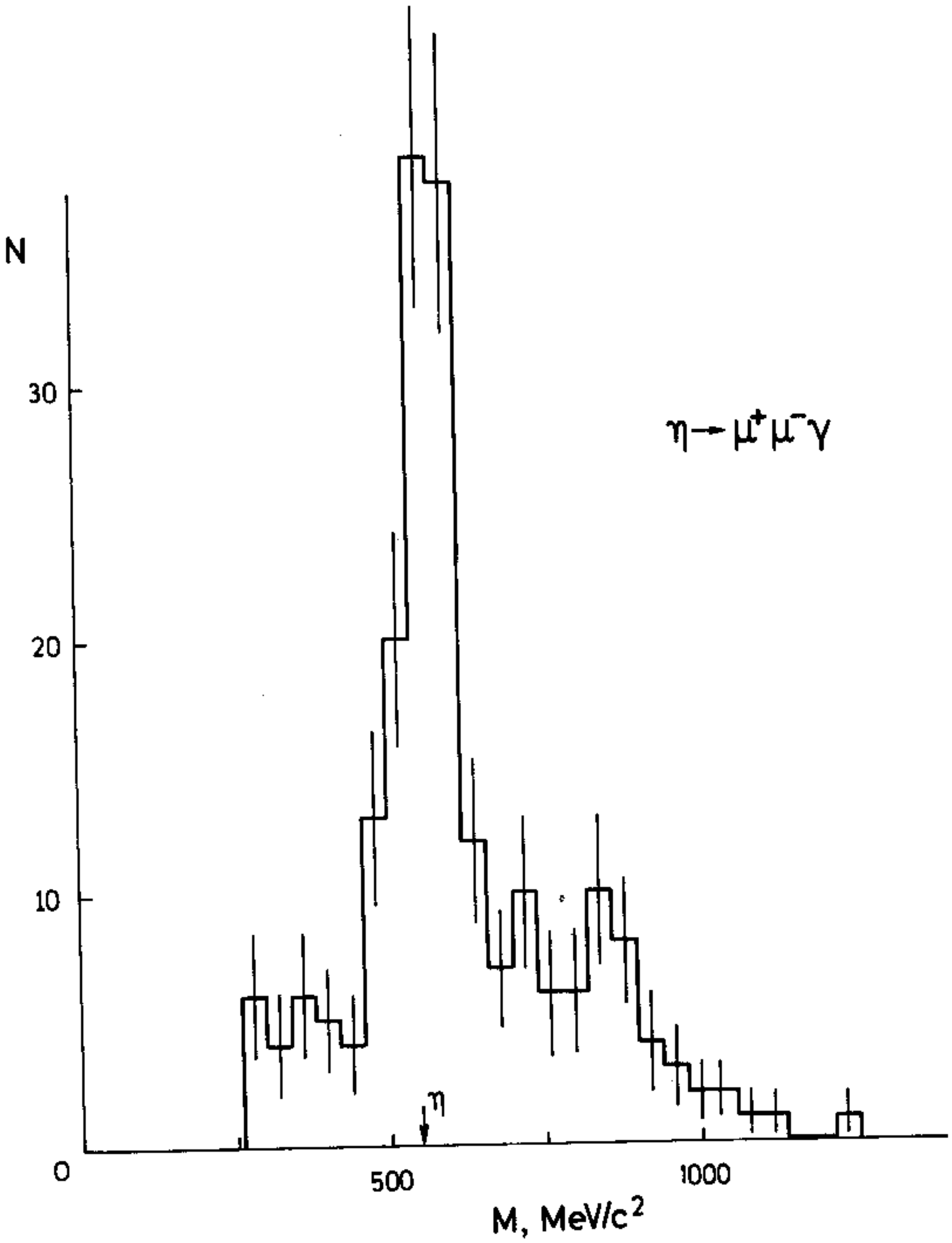

Fig. 17